

## Competition between magnetic and superconducting pairing exchange interactions in confined systems

Zu-Jian Ying,<sup>1,2,3</sup> Mario Cuoco,<sup>1,2</sup> Canio Noce,<sup>1,2</sup> and Huan-Qiang Zhou<sup>3,4</sup>

<sup>1</sup>Laboratorio Regionale SuperMat, INFN-CNR, I-84081 Baronissi, Salerno, Italy

<sup>2</sup>Dipartimento di Fisica "E. R. Caianiello," Università di Salerno, I-84081 Baronissi, Salerno, Italy

<sup>3</sup>Department of Physics, Chongqing University, Chongqing 400044, People's Republic of China

<sup>4</sup>School of Physical Sciences, The University of Queensland, Brisbane Qld 4072, Australia

(Received 8 September 2007; published 24 October 2007)

We analyze the competition between magnetic and pairing interactions in confined systems relevant to either small superconducting grains or trapped ultracold atomic gases. The response to the imbalance of the chemical potential for the two spin states leads to various inhomogeneous profiles of the pair energy distribution. We show that the position in the energy spectrum for the unpaired particles can be tuned by varying the filling or the pairing strength. When small grains are considered, the antiferromagnetic exchange stabilizes the pair correlations, whereas for Fermi gases, a transition from a mixed configuration to a phase-separated one beyond a critical polarization threshold appears, as does an unconventional phase with a paired shell around a normal core.

DOI: [10.1103/PhysRevB.76.132509](https://doi.org/10.1103/PhysRevB.76.132509)

PACS number(s): 74.20.Fg, 03.75.Hh, 75.75.+a

The nature of paired quantum configurations has received a great deal of attention, especially in confined systems such as small superconducting (SC) grains<sup>1,2</sup> and in optical traps for cold atoms.<sup>3-5</sup> The recent achievements both in the field of nanoscale devices and in the area of ultracold fermionic gases provide playgrounds to test pair correlated states with several tunable control parameters. Special features may be generated when the chemical potentials of the two spin (atomic) states are not equal, as they occur by including a spin-only applied field, mass asymmetry, and unequal density populations.<sup>5,6</sup> Pairing (PA) is usually modified, or eventually broken down, due to the Fermi energy mismatch. In such a case, unpaired (normal) configurations may coexist with paired ones under various inhomogeneous forms.<sup>5,7,8</sup> Nevertheless, the condition for the coexistence of strong pair correlations (PCs) and unpaired normal states is hardly met in these systems.

In this Brief Report, we analyze in detail the competition between magnetic and PA exchange in the presence of spin imbalance within confined systems relevant to either small SC grains or trapped ultracold atomic gases. For small SC grains, due to the attractive electron-electron interaction, the PA and antiferromagnetic (AFM) exchange are the leading coupling terms.<sup>9,10</sup> The AFM interaction in such systems, or in AFM metallic clusters, is enhanced and can even be much larger than the level spacing.<sup>10,11</sup> This provides a different scenario from the case of small metallic dots where the electron interaction leads to an exchange of ferromagnetic type.<sup>9,12,13</sup> In such a context, our analysis suggests a practical way to achieve a ground state (GS) in which *strong* PCs coexist with a normal configuration. Furthermore, we show how to manipulate the unpaired spectrum concerning its position within the pair distribution function (PDF). The microscopic ingredients we need to take into account are (i) the competition between the PA interaction and a mechanism of spin quenching, (ii) the size of the system, (iii) the electron density, and (iv) a mechanism to unbalance the energy of the two spin states. To this end, we use a universal model

Hamiltonian<sup>9,10</sup> in the presence of a magnetic field. The energy imbalance between the two spin states drives the system toward a two-component configuration. The conventional wisdom yields a spectrum of polarized electrons lying around the effective Fermi level<sup>1</sup> and the pairs mainly occupying the lowest energy levels with a small tail above the unpaired (blocked) sector, due to coexisting weak PCs. We shall show that this picture is modified when the spin exchange softens the depairing processes. For small SC grains, this effect leads to the coexistence of strong PCs and unpaired electrons whose energy spectrum moves within the paired sector and even resides at the bottom of the band. In the context of atomic Fermi gases, our analysis indicates a possible mechanism for the transition from a mixed configuration to a phase-separated one, tuned by the increase of the polarization. Under special conditions of PA and filling, another type of phase-separated state emerges with an unpaired core surrounded by paired fermions.

*Description of the model.* The dynamics we refer to can be described by the following Hamiltonian:

$$H = \sum_{j,\sigma} \varepsilon_j c_{j\sigma}^\dagger c_{j\sigma} - g \sum_{j,j'} c_{j+}^\dagger c_{j-}^\dagger c_{j'-} c_{j'+} - J \hat{S}^2 - h \hat{S}^z, \quad (1)$$

where  $c_{j\sigma}^\dagger$  ( $c_{j\sigma}$ ) is the creation (annihilation) operator for an electron on a discrete single-electron energy level  $\varepsilon_j$ . The second and third terms of  $H$  stand for the PA interaction and the AFM spin exchange ( $J < 0$ ), respectively. The last contribution to  $H$  is the Zeeman energy with a magnetic field  $h$  in the  $z$  direction, acting as a chemical potential spin imbalance. The AFM exchange is the Casimir operator of the SU(2) Lie algebra in spin sector, with  $\hat{S}_j^+ = (\hat{S}_j^-)^\dagger = c_{j+}^\dagger c_{j-}$  and  $\hat{S}_j^z = (c_{j+}^\dagger c_{j+} - c_{j-}^\dagger c_{j-})/2$ . Hamiltonian (1) is exactly solvable<sup>14</sup> (see also Refs. 15 and 16). The singly occupied levels do not participate in the pair scattering, thus staying "blocked" according to the Pauli principle. In the presence of  $n$  pairs in unblocked levels  $\Omega_U$  and a total spin  $S$  from the blocked ones  $\Omega_B$ , the eigenenergy  $E = \sum_{\mu=1}^n E_\mu - S(S+1)J - hS^z + \sum_{j \in \Omega_B} \varepsilon_j$  is deter-

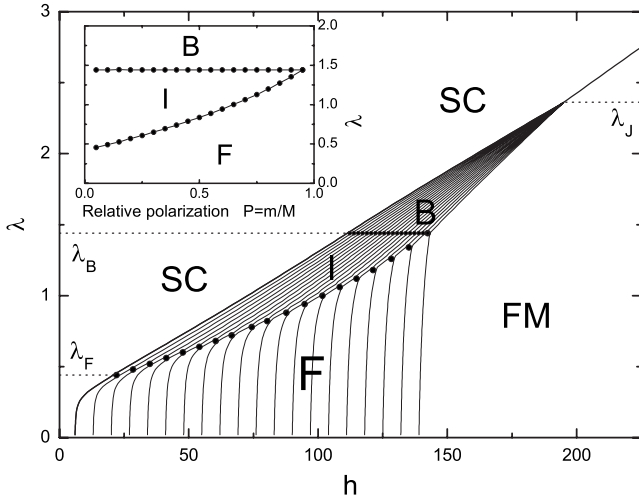


FIG. 1. Ground state diagram in the pairing-strength/field ( $\lambda, h$ ) plane for 40 electrons over 100 levels at a spin exchange  $J = -2.5d$ . The electrons are all paired in the SC region and fully polarized in the FM region, while partially polarized electrons reside around the Fermi level (F), inside the paired sector (I), or at the bottom of the band (B). Inset: Ground state diagram expressed in terms of the polarization  $P$ .

mined by the equation<sup>14</sup>  $\frac{1}{g} + \sum_{\nu=1}^n \frac{2}{\nu(\nu+\mu)} \frac{1}{E_\nu - E_\mu} = \sum_{j \in \Omega} \frac{1}{2E_j - E_\mu}$ . The breakdown of  $m$  pairs gives rise to a spin SU(2) multiplet with the constraint  $m \geq S \geq |S^z|$ . Although the spin exchange is AFM, the GS exhibits the highest spin projection  $S^z = S = m$ . Indeed, when  $S$  is given for a fixed spin exchange energy, the field favors  $S^z = S$ , while the GS has the smallest number of broken pairs ( $m = S$ ) due to the PA term. The most stable state is obtained by comparing the energy of all possible pair breaking and spin configurations. Here, our application involves  $N$  total electrons for an energy spectrum  $\epsilon_j = jd$ ,  $j = 1, \dots, \Omega$ , with the total level number fixed ( $\Omega = 100$ ) and  $d$  being the mean level spacing. We notice that for larger values of  $\Omega$ , no significant changes in the qualitative behavior of the field response are observed. The parameters  $J$ ,  $g$  ( $\lambda = g/d$ ), and  $h$  are scaled by  $d$ . As a general strategy, we first analyze a specific filling and then present the results for various electron densities.

*Ground state diagram and the spectrum of the unpaired electrons.* The GS diagram in  $(h, \lambda)$  plane is plotted in Fig. 1, for a filling of 40 electrons and  $J = -2.5d$ . Depending on the character of the GS configurations, various regions may be identified: (i) a configuration SC with superconducting PCs, i.e., no polarized electrons exist; (ii) a partially polarized region (PP-SC) where PCs come together with blocked configurations labeled with F, B, and I, which are identified by considering whether the position of the blocked sector lies around the uncorrelated Fermi level (F), at the bottom of the band (B), or inside the paired sector (I); and (iii) a fully polarized ferromagnetic (FM) configuration. The solid lines in the PP-SC region separate the GS configurations with different numbers of broken pairs that grow with the field until they reach the FM configuration. The sparse (dense) boundaries within the PP-SC area distinguish two regimes driven by the field, and the GS in this regime exhibits unusual features as far as the PDF is concerned.

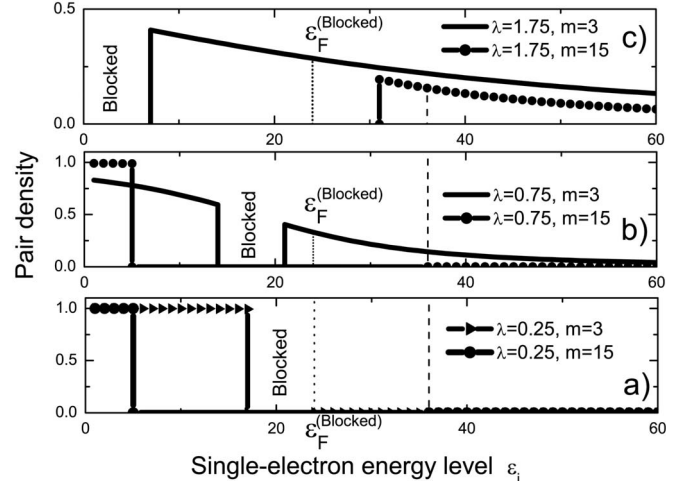


FIG. 2. Pair distribution function at  $J = -2.5d$  with 40 electrons for different values of the pairing exchange  $\lambda$  and of the number of polarized pairs  $m$  in the GS. The dotted line indicates the uncorrelated Fermi level  $\epsilon_F^{(Blocked)}$ .

Before discussing in detail the GS diagram in Fig. 1, it is worthwhile pointing out a few aspects related to the strength of the magnetic coupling. For an AFM exchange weaker than a threshold  $J_B \cong -1.68d$ , the field amplitude  $h$  at the boundary between the FM and the PP-SC regions is insignificantly affected by changes in  $\lambda$ . For  $J < J_B$  and independent of  $J$ , when the PA coupling overcomes  $\lambda_B \cong 1.45$  (see Fig. 1), there is a fast growth of the critical field between the FM and the PP-SC regions. It is such a change in the behavior of the field response that characterizes another type of PC in the GS that is referred to as the B region.

*Analysis for the pair distribution function profiles.* In Fig. 2, we show typical behaviors of PDF profiles. The profiles turn out to be completely different depending on the value of the pair coupling. Indeed, we can classify three regimes: (a)  $\lambda < \lambda_F$ , (b)  $\lambda_F < \lambda < \lambda_B$ , and (c)  $\lambda_B < \lambda < \lambda_J$ . In (a), the field drives the GS into the F region of the GS diagram in Fig. 1, which is characterized by weak PCs. The PDF as shown in Fig. 2(a) has a unit-step-like structure, with all of the discrete levels almost doubly occupied below an effective Fermi level; then, a gap, whose size depends on the number of broken pairs, appears, followed by a tail with a very small weight, reflecting the weak but long-range character of the PCs. In this PA regime, a change in the field amplitude, which increases the broken pairs, does not modify the PDF shape.

In (b), the PDF profile exhibits essentially different features in low and high polarizations. For a small number of broken pairs, there is a significant weight above the blocked sector. This implies that the PCs are strong, so the interlevel exchange dominates over the intralevel exchange and the pairs get more homogeneously distributed over the entire spectrum. As shown in Fig. 2(b), the polarized electrons “sink” down toward the bottom of the energy band away from the Fermi level; therefore, they are completely embedded in the paired configurations. In this regime, simply by increasing the field amplitude, the system is driven to undergo a changeover from uniform distribution to steplike dis-

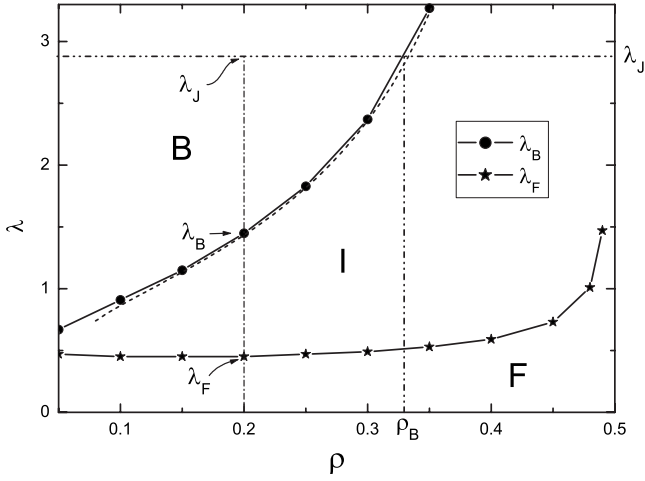


FIG. 3. Evolution of the position of the blocked sector vs  $\lambda$  and density  $\rho$  of electrons (holes) below (above) half-filling. The dashed line is the analytical result for  $\lambda_B$ .  $\lambda_B$  and  $\lambda_F$  at  $\rho=0.2$  are the same as in Fig. 1, while  $\lambda_J$  increases with  $|J|$ .

tribution in the PDF profile. Indeed, when the boundary between the I and the F regions is crossed, the PDF weight transfers from the high energy levels to the lower ones, indicating a transition from strong PCs to weak PCs.

In (c), an unconventional position of the spectrum of unpaired electrons characterizes region B: all of the broken pairs fill the lowest energy levels, while the PDF profile is nearly uniform over the rest of the band [see Fig. 2(c)]. Since paired and unpaired electrons are now completely segregated, there is no blocked sector separating the two paired sectors as in cases (a) and (b). This makes it possible for the maximally permitted PCs to coexist with a finite spin polarization. Moreover, in this regime, the PDF profile is always robust against the applied field, in the sense that the increase of unpaired electrons does not weaken the PCs since they remain unaffected until all pairs break down.

*Manipulating the pair correlation strength and the pair distribution function profiles.* To illustrate clearly how the spectrum of unpaired electrons is modified, we plot  $\lambda_B$  and  $\lambda_F$  as a function of the total electron density in Fig. 3 [ $\rho \equiv N/(2\Omega)$ ]. The diagram in the  $(\rho, \lambda)$  plane is separated into three regions F, I, and B due to the position of the blocked sector. The spin polarization in these regions generally starts with a process of single pair breaking if the PA exchange is below  $\lambda_J$  (horizontal dotted line). For  $\lambda$  larger than  $\lambda_J$ , the pair breaking involves a magnetization jump to full (large) polarization for a filling below (above)  $\rho_B$ . In Fig. 3,  $\rho_B$  is labeled by the crossing points of  $\lambda_B$  and  $\lambda_J$ . In regime B, where  $\rho < \rho_B$  and  $\lambda \in [\lambda_B, \lambda_J]$ , all the unpaired electrons are located at the bottom of the band. The explicit value of  $\rho_B \equiv (d+J)/(2J)$ , valid for  $J < -1.2d$ , can be obtained by solving the equation  $\lambda_B = \lambda_J$ . In a similar way, given an electron (hole) density below (above) half-filling, the B regime occurs for  $J < J_B \equiv -d/(1-2\rho)$ . The analytic dependence of  $\lambda_B$  on the density can be determined by combining expansions at strong<sup>17</sup> (weak<sup>18</sup>) coupling in  $\lambda$  for the B (F) regime, as in Ref. 19. This yields  $\lambda_B \approx \{1 + \sqrt{[16\rho(1-\rho) - 1]/3}\}/$

$[2(1-2\rho)]$ . Also,  $\lambda_J \approx \frac{1}{2d}(|J| + \sqrt{J^2 - \frac{4}{3}d^2})$  is independent of the filling but varies with the exchange amplitude. As illustrated in Fig. 3, by varying the filling or the scaled PA strength, one can manipulate the position of the spectrum of unpaired electrons from the F to I and B regimes.

*Basic mechanisms.* Let us now consider a simple physical picture to explain how the position of the blocked sector can be tuned over the entire spectrum. Qualitatively, such a phenomenon can be understood in terms of the occupation profile versus the energy. For weak PCs, the pairs tend to fill up the available states from the bottom of the band. Then, the given number of depaired single electrons will stay within the blocked levels at energies above the doubly occupied states. When  $\lambda$  grows, the pairs can escape the blocking of the unpaired sector and occupy the previously empty levels. Hence, the strong PA regime leads to an almost homogeneous PDF in the unblocked sector.

For densities below half-filling, the tendency to form a uniform pair distribution leads to an average occupation lower than one electron per energy level. On the other hand, the single-electron configurations do not feel charge fluctuations, thus having a fixed occupation number equal to one electron per energy level. Hence, due to the peculiar density profile, it is more favorable to fill the lower energy levels with singly occupied configurations rather than paired ones. The emerging picture is that the single electrons appear *heavier* than the pairs so that the blocked sector moves down toward the bottom of the band. In the regime of strong PCs and a dilute filling, all the pairs get “lighter” than the single electrons so that the full blocked sector is located at the bottom of the band. Therefore, by adapting the PA strength, or by tuning the filling factor, it is possible to control the PDF profile and in turn the spectrum of unpaired electrons. Most interestingly, once regime B is reached, breaking more pairs makes them more dilute over the unblocked levels, since the average pair density  $\rho_m = (M-m)/(\Omega-2m)$  ( $M = N/2$  is the maximum pair number) gets smaller with increasing broken pair number  $m$  for densities below half-filling  $N < \Omega$ . Hence, the pairs get even lighter after each depairing and consequently always stay above the unpaired electrons. As a result, the strong PC in regime B is not hindered by any depairing processes.

Let us now point out the role of the magnetic exchange  $J$ . As seen above, the manipulation of the PDF occurs in the regime where strong PCs can be adjusted with a nonzero density of polarized electrons. Such a possibility occurs only when the AFM amplitude overcomes a critical threshold. Indeed, in the absence of AFM coupling and within a regime of strong PA, hopping of the  $(M-m)$  pairs to  $\Omega-M-m$  empty levels, together with the intralevel pair contribution, gives  $E_m^g \sim -(M-m)(\Omega-M-m+1)g$  at the leading order for the total energy. The average cost for breaking  $m$  pairs is then  $(E_m^g - E_0^g)/m \sim (\Omega-m+1)g$ . This implies that the largest possible  $m$  is the most favorable, and so the paired state breaks down, indicating the difficulty for the coexistence of strong PCs and a finite polarization. The spin exchange coupling, on the other hand, counteracts such a tendency, as it leads to a minimization of pair breaking by introducing an additional average energy cost  $\sim -J(m+1)$ . Thus, for the AFM ex-

change stronger than the leading-order value of the threshold  $-g$ , an inversion of the behavior of the pair breaking energy cost occurs so as to soften the depairing processes. Therefore, it is the subtle competition between the magnetic and PA exchange couplings that opens the route to the spectral tunability of the PDF profile.

At this point, it is useful to discuss the size dependence of  $\lambda$  in granular superconductors. For phonon-mediated superconductors, two mechanisms involve the variation of  $\lambda$ : ( $\alpha$ ) the softening of the phonon spectrum<sup>20</sup> and ( $\beta$ ) the change of the density of states due to the discretization of the bands.<sup>21</sup> When the particle size is reduced,  $\alpha$  leads to an enhancement of  $\lambda$ , while  $\beta$  tends to suppress the PA coupling.<sup>23,24</sup> Thus, two scenarios can occur for  $\lambda$ : decreasing from the bulk value to a small amplitude and being enhanced before getting suppressed. Considering intermediate-coupling superconductors (e.g., Sn, Nb, and In with bulk values of  $\lambda$  between 0.5 and 0.8),<sup>22</sup> one can observe the I-like configuration, and in the ultrasmall limit, the field response would lead to a transition from SC to a F-like state due to the  $\beta$  mechanism. For strong-coupling superconductors, such as Pb ( $\lambda \sim 1.55$ ),<sup>22</sup> a transition from SC to B can be obtained at first, and then below a critical size from SC to I- or F-like configurations. We speculate that a similar behavior would occur in high temperature superconductors, as they are in a regime of strong coupling and the AFM exchange ( $\sim 80$  meV) is larger than an average estimate, via the Kubo expression,<sup>25</sup> for the level spacing ( $d \sim 7$  meV) in nanoparticles. For non-phonon-mediated superconductors, the variation of  $\lambda$  may be more involved due to the lack of detailed *ab*

*initio* microscopic information about the PA mechanism.

*Relevance to atomic Fermi gases.* We discuss a possible application to the two spin state mixture of ultracold atomic gases in optical traps. Recent experiments have demonstrated the possibility for a phase separation driven by tuning the unbalanced state populations.<sup>5</sup> In the context of atomic Fermi gases, the lower (higher) energy levels correspond to configurations of atoms that are closer to (farther away from) the inner core of the trap, as selected by their smaller (larger) kinetic energy. Thus, the GS configuration in regime F represents a phase with a paired core surrounded by a shell of normal unpaired atoms, while the high energy pair tail can be neglected due to the extremely small PDF weight. Interestingly, for the GS configuration in regime I, the PDF is more uniform both below and above the blocked sector, which in turn results in a smaller energy cost for the unpaired atoms to exist separately among the pairs. Therefore, unpaired and paired atoms appear to be more hybridized at very low temperatures. Moreover, in regime F, the energy cost for unpaired-paired mixing is much higher due to the extreme imbalance of the PDF below and above the blocked sector, leading to a clear separation of paired and normal atoms. Then, as shown in Figs. 1 (inset) and 2(b), a high polarization drives a changeover from regime I to regime F, which indicates a transition from a mixed phase to a phase-separated configuration. Such case may be relevant for the scenario addressed in Ref. 5. Finally, region B provides another kind of phase separation, in which the inner core is composed of unpaired atoms, with the shell formed by pairs.

- 
- <sup>1</sup>J. von Delft and D. C. Ralph, Phys. Rep. **345**, 61 (2001), and references therein.
- <sup>2</sup>D. C. Ralph, C. T. Black, and M. Tinkham, Phys. Rev. Lett. **74**, 3241 (1995).
- <sup>3</sup>C. Chin, M. Bartenstein, A. Altmeyer, S. Riedl, S. Jochim, J. Hecker Denschlag, and R. Grimm, Science **305**, 1128 (2004).
- <sup>4</sup>M. W. Zwierlein, J. R. Abo-Shaeer, A. Schirotzek, C. H. Schunck, and W. Ketterle, Nature (London) **435**, 1047 (2005).
- <sup>5</sup>G. B. Partridge, W. Li, R. I. Kamar, Y. Liao, and R. G. Hulet, Science **311**, 503 (2006).
- <sup>6</sup>R. Casalbuoni and G. Nardulli, Rev. Mod. Phys. **76**, 263 (2004).
- <sup>7</sup>P. Fulde and R. Ferrel, Phys. Rev. **135**, A550 (1964); A. Larkin and Y. Ovchinnikov, Sov. Phys. JETP **20**, 762 (1965).
- <sup>8</sup>W. V. Liu and F. Wilczek, Phys. Rev. Lett. **90**, 047002 (2003).
- <sup>9</sup>I. L. Kurland, I. L. Aleiner, and B. L. Altshuler, Phys. Rev. B **62**, 14886 (2000).
- <sup>10</sup>P. San-Jose, C. P. Herrero, F. Guinea, and D. P. Arovas, Eur. Phys. J. B **54**, 309 (2006).
- <sup>11</sup>B. Mühlischlegel, D. J. Scalapino, and R. Denton, Phys. Rev. B **6**, 1767 (1972).
- <sup>12</sup>M. N. Kiselev and Y. Gefen, Phys. Rev. Lett. **96**, 066805 (2006).
- <sup>13</sup>I. Aleiner, P. Brouwer, and L. Glazman, Phys. Rep. **358**, 309 (2002).
- <sup>14</sup>R. W. Richardson, Phys. Rev. **141**, 949 (1966); J. Math. Phys. **18**, 1802 (1977).
- <sup>15</sup>H.-Q. Zhou, J. Links, R. H. McKenzie, and M. D. Gould, Phys. Rev. B **65**, 060502(R) (2002).
- <sup>16</sup>Z.-J. Ying, M. Cuoco, C. Noce, and H.-Q. Zhou, Phys. Rev. B **74**, 012503 (2006).
- <sup>17</sup>E. A. Yuzbashyan, A. A. Baytin, and B. L. Altshuler, Phys. Rev. B **68**, 214509 (2003).
- <sup>18</sup>M. Schechter, Y. Imry, Y. Levinson, and J. von Delft, Phys. Rev. B **63**, 214518 (2001).
- <sup>19</sup>Z.-J. Ying, M. Cuoco, C. Noce, and H.-Q. Zhou, Phys. Rev. B **74**, 214506 (2006).
- <sup>20</sup>J. M. Dickey and A. Paskin, Phys. Rev. B **1**, 851 (1970).
- <sup>21</sup>M. Strongin, R. S. Thompson, O. F. Kammerer, and J. E. Crow, Phys. Rev. B **1**, 1078 (1970).
- <sup>22</sup>P. B. Allen and R. C. Dynes, Phys. Rev. B **12**, 905 (1975).
- <sup>23</sup>S. Bose, P. Raychaudhuri, R. Banerjee, P. Vasa, and P. Ayyub, Phys. Rev. Lett. **95**, 147003 (2005).
- <sup>24</sup>W.-H. Li, C. C. Yang, F. C. Tsao, and K. C. Lee, Phys. Rev. B **68**, 184507 (2003).
- <sup>25</sup>R. Kubo, J. Phys. Soc. Jpn. **17**, 975 (1962).